

A Study of LPM Suppression of Bremsstrahlung at 25 GeV.*

The SLAC E-146 Collaboration

P. Anthony^a, R. Becker-Szendy^b, P. Bosted^c, M. Cavalli-Sforza^d, L. Keller^b,
 L. Kelley^d, S. Klein^d, G. Niemi^b, M. Perl^b, L. Rochester^b, J. White^c

a: Lawrence Livermore National Laboratory, Livermore, CA. 94550, USA

b: Stanford Linear Accelerator Center, Stanford University, Stanford, CA. 94305, USA

c: The American University, Washington D.C., 20016, USA

*d: Santa Cruz Institute for Particle Physics University of California, Santa Cruz, CA.
 95064 USA*

Abstract

We are making an accurate measurement of the LPM suppression of bremsstrahlung with 25 GeV electrons. By using a 120 pulses per second beam, a precise BGO calorimeter, and spectrometer to tag the outgoing electrons, we are able to make an accurate measurement of the bremsstrahlung photons in the 0-400 MeV region, where the Bethe Heitler and LPM predictions differ. We are taking data with targets made of carbon, uranium, tungsten and iron, with thicknesses in the 2% to 6% X_0 range. In addition, we are taking data with two very thin gold targets. The latter have thicknesses that are comparable to or less than the LPM formation zone length, and so should not exhibit LPM suppression. We are also studying photons of a few MeV in energy, to test the closely related longitudinal density effect predicted by Ter-Mikaelian in which very low energy photon emission is suppressed due to dielectric effects of the medium.

1. Introduction

In the early 1950's, it was realized that, in contrast to the classical picture, bremsstrahlung is not a point interaction¹. When a high energy electron exchanges a virtual photon with a nucleus and emits a photon via bremsstrahlung, the longitudinal momentum transfer between the electron and the nucleus is very small²

$$q_{\parallel} \sim \frac{m^2 E_{\gamma}}{2E_e(E_e - E_{\gamma})} \sim \frac{E_{\gamma}}{2\gamma^2}$$

where γ is E_e/m , and the latter relationship only holds for $E_{\gamma} \ll E_e$. Because q_{\parallel} is small, by the uncertainty principle, the exchange must take place over a finite distance, h/q_{\parallel} . If something happens to the electron while it traverses this distance, the emission is suppressed.

A number of processes can perturb the electron and so suppress the bremsstrahlung. In the LPM effect, if the electron scatters by an angle larger than the photon emission angle $1/\gamma$, then the emission is suppressed. This happens when the photon energy is less than E_e^2/E_{LPM} , where E_{LPM} is a material dependent constant, 2.6 TeV in uranium and 4.2 TeV in lead. For example, for a 25 GeV electron in uranium, the suppression is significant for photon energies below 250 MeV. Figure 1 compares the Bethe-Heitler spectrum with the results of a detailed LPM calculation³ for 25 GeV electrons in uranium.

*Work supported by Department of Energy contract DE-AC03 76SF00515.

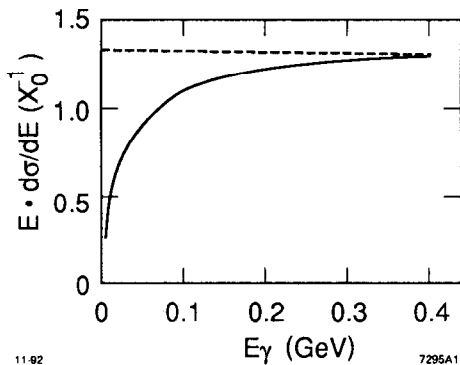


Fig. 1. Comparison of the LPM (solid line) and Bethe Heitler (dashed line) bremsstrahlung cross sections for 25 GeV electrons in uranium.

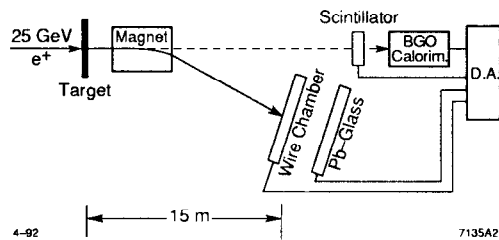


Fig 2. Layout of the proposed experiment. The scintillator is used to veto charged particles hitting the calorimeter. is due to synchrotron radiation from the spectrometer magnet.

A similar process affects pair creation by high energy photons. Because the LPM effect depends on the electron energy, the effect influences photon conversions only at higher energies. At high enough energies, the LPM effect increases the effective radiation length, lengthening electromagnetic showers.

For low energy bremsstrahlung photons, another phenomenon, the longitudinal density effect, becomes important.⁴ In it, the dielectric constant of the medium gives the photon a phase shift over the length of the formation zone. Then, contributions to the photon amplitude from different portions of the formation zone stop adding coherently, reducing the photon amplitude. This occurs when $\exp(i(k \cdot x - \omega t))$ changes significantly over the formation zone, which happens when $k \cdot x - \omega t \approx 1$ for $x = l = ct$. Here $k = \sqrt{\epsilon\omega}/c = \omega/c\sqrt{1 - \omega^2/\omega_p^2}$ where ω_p is the plasma frequency (60-80 eV in dense media). Some algebra shows that this effect is significant for photon energies below $\gamma\omega_p$, which occurs for $E_\gamma/E_e < \omega_p/m_e$, which is 1.4×10^{-4} in uranium and 5.5×10^{-5} in carbon. For 25 GeV electrons, the dielectric effect appears for photon energies below 3.5 MeV and 1.4 MeV respectively.

Previous experiments have studied the LPM effect qualitatively. Most of the experiments have used cosmic rays to study the LPM effect on pair production. In 1977, a group at Serpukhov studied the LPM effect on bremsstrahlung using 40 GeV electrons. They saw a somewhat larger effect than predicted by theory, but with large systematic uncertainties⁵

2. Experimental Apparatus

The experimental apparatus, shown in Figure 2, is located in End Station A at SLAC. A low intensity (single e^-) beam hits a thin target, emitting a photon which travels downstream into a BGO calorimeter. The electrons are bent by a dipole magnet into a wire chamber which measures the electron deflection, and thus its momentum.

The calorimeter consists of 45 BGO crystals, each measuring 2 cm square by 20 cm ($18 X_0$) deep. It produces 100-150 photoelectrons per MeV, and has an energy resolution of 8% FWHM at 40 MeV. The calorimeter is 50 meters downstream from the target, giving an angular resolution of 0.1 mrad, allowing us to study the angular dependence of the LPM effect. Since the BGO light output varies with temperature, the calorimeter temperature is monitored with a thermistor.

The 3.25 Tesla-meter magnet bends 25 GeV electrons by 40 mrad. Its relatively large fringe field starts the electron bending slowly, so relatively little synchrotron radiation hits the central area of the calorimeter. Six wire chamber planes are located 15 meters downstream from the magnet to track the electrons. The 2 mm pitch wires measure electron momentum to 27 MeV/c, less than the uncertainty due to multiple scattering in the targets. Behind the wire chambers are lead glass blocks. They provide a simple calorimetric way to count electrons on a pulse by pulse basis.

The experiment requires a low intensity (1 electron/pulse) beam. The beam is produced parasitically from off axis electrons in the SLAC linear accelerator, while the main beam is being used for e^+e^- collisions. During normal operations, about 10% of the SLC beam is scraped off by collimators at the end of the linac. Since the collimators are relatively thin ($2.2 X_0$), some high energy photons escape from the collimators and continue downstream into the beam switchyard. There, they hit a $0.7 X_0$ production target and are converted into e^+e^- pairs. The electrons are captured by the A-line and transported to the end station. Beam fluxes range up to 100 electrons/pulse, depending on the A-line collimator settings. At 1 electron/pulse, the beam size (1σ) is 4 mm \times 2.4 mm, with angular divergence less than 0.05 mrad. and an energy spread of 0.1% full width. During data taking, the beam size is monitored periodically with a 1 cm square silicon diode that serves as an active target.

3. Running Plan

We will take data with five target materials: carbon, iron, lead, tungsten, and uranium, in two thicknesses for each target. The target thicknesses range between 2% and 6 % of X_0 . These thicknesses are a tradeoff between a high rate and pileup from a single electron interacting twice in the target. The two thicknesses per material provide a check of our understanding of the remaining multiphoton pileup.

Runs with an empty target holder have shown that beam related backgrounds to bremsstrahlung are small. As discussed above, little synchrotron radiation, a potential background below 1 MeV, hits the center of the calorimeter. Target related backgrounds are also small. The relative cross section for electronuclear reactions is small, and mostly removed by constraining the total observed energy to the beam energy. There is a small background from transition radiation as the electrons traverse the target. Although the transition radiation intensity is low, the photon spectrum extends up to $\gamma\omega_p$, the same energy at which the longitudinal density effect occurs.

At the time of this writing, we are in the midst of data taking. Our plan is to collect 16 hours of data for each target material (corresponding to about 3 million single electron events) and 8 hours for the thick targets. In addition to

taking data at 25 GeV, we will also run at 8 GeV, where the LPM onset energy is a factor of 10 lower. This will serve as a systematic check of the experiment and the LPM effect.

Since the bremsstrahlung spectrum is proportional to $1/E_\gamma$, it is convenient to bin data logarithmically in energy, so each bin has a similar number of counts. For our data and a bin width $\Delta E = 0.1E$, the statistical accuracy is better than 2%. Thus, we expect to be limited by systematic errors. In addition to the 8 GeV running mentioned above, we have a number of other experimental checks. Target thickness effects are studied by Monte Carlo simulation and by taking data at two target thicknesses. The BGO calorimeter resolution is well known from a series of beam tests⁶.

Our largest systematic effect is likely to be the absolute BGO energy calibration. This is monitored in 4 ways: At low energies, we use radioactive sources and cosmic rays. At LPM energies, we will cross calibrate the calorimeter with the wire chamber. Finally, we will attempt to run a low energy (300-500 MeV) electron beam directly into the calorimeter.

In addition to the standard targets, we will take data with two gold targets with thicknesses 1% and 0.1 % of X_0 . These targets have thicknesses comparable to the formation zone length, and should not exhibit the LPM effect.

4. Conclusions

We are in the midst of taking data which will allow us to make a high precision test of the LPM effect with 25 GeV electrons. Based on a preliminary look, the data quality appears excellent, and we will present a full report in Calgary.

Acknowledgments

We would like to thank the SLAC accelerator operations and EFD groups for their excellent technical support. In particular, Roger Erickson, Roger Gearhart and Steve St. Lorant have provided invaluable assistance. In addition, we would like to thank Al Odian for suggesting the parasitic beam concept to us.

References

1. M. Cavalli-Sforza, *et al.*, SLAC-Proposal-E-146, June 15, 1992.
2. L. D. Landau and I.J. Pomeranchuk, *Dokl. Akad. Nauk. SSSR* **92**, 535 (1953); **92**, 735 (1953). These two papers are available in English in L. Landau, *The Collected Papers of L.D. Landau*, Pergamon Press, 1965. See also E.L. Feinberg and I. Pomeranchuk, *Nuovo Cimento*, Supplement to Vol **3**, 652 (1956).
3. A.B. Migdal, *Phys. Rev.* **103**, 1811 (1956).; T.Stanev *et al.*, *Phys. Rev.* **D25**, 1291 (1985).
4. M.L. Ter-Mikaelian, *Dokl. Akad. Nauk. SSR* **94**, 1033 (1954). For a discussion in English, see M.L. Ter-Mikaelian, *High Energy Electromagnetic Processes in Condensed Media*, John Wiley & Sons, 1972.
5. A. Varfolomeev *et al.*, *Sov. Phys. JETP* **42**, 218 (1976).
6. I. Kirkbride, the SLAC Users Bulletin No 97, Jan-May, 1984, pp 10-11.